Joint Pathology Center
Veterinary Pathology Services

WEDNESDAY SLIDE CONFERENCE 2025-2026

Conference #21 08 April 2026

Case 1:

Signalment:

5-year-old, neutered male, domestic ferret (*Mustela putorius furo*)

History:

The patient was presented to the Exotics Service for evaluation of acute non-ambulatory paraparesis. The patient had a more prolonged history of lethargy and diarrhea. Neurolocalization was to the T3-L3 spinal cord. On abdominal palpation, the bladder was markedly distended and turgid; the spleen was severely enlarged, and multiple abdominal lymph nodes were enlarged. Cytology of the spleen showed moderate plasmacytosis and extramedullary hematopoiesis. The owners elected euthanasia due to concerns for quality of life.

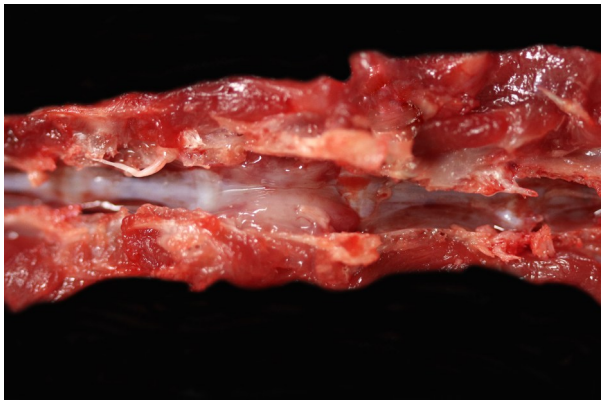

Figure 1-1: Spinal column, ferret: A 0.6cm long, soft, light purple grey, bilobed mass arises from the ventral vertebral body of T11 and protrudes into the spinal canal. (*Photo courtesy of*: Schwarzman Animal Medical Center, 510 East 62nd St. New York, NY 10065. http://www.amcny.org)

Gross Pathology:

Associated with the vertebral body and the ventral aspects of the pedicles of T11 and protruding into the vertebral canal was a 0.6 cm long, soft, light purple grey, bilobed mass that surrounded and compressed the local segment of spinal cord. With examination of the external surface, an approximately 1.4 cm long segment of the regional spinal cord was streaked white, red, and dark red (hemorrhages). After formalin fixation and decalcification, the T11-L1 vertebrae was sectioned serially. The cut surfaces of the T11 vertebral body and portions of the pedicles were expanded and replaced by a poorly demarcated, soft, shiny, white tissue inconsistently mantled by an irregular brown rim that filled the medullary cavity with loss of the trabecular architecture. The regional cortical bone was irregular and multifocally thinned.

In addition, the spleen was severely enlarged (95.6 g; 6.8% of the body weight) with dozens of randomly distributed sharply demarcated, pinpoint to 0.6 cm in diameter, oval to spherical, soft, white foci and nodules.

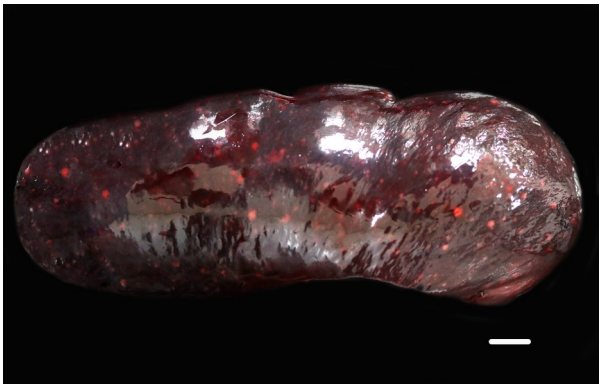

Figure 1-2: Spleen, ferret: There is marked splenomegaly and the parenchyma contains numerous cellular foci ranging up to 0.6cm in diameter. (*Photo courtesy of*: Schwarzman Animal Medical Center, 510 East 62nd St. New York, NY 10065. http://www.amcny.org)

Laboratory Results:

Pertinent Hematology and Biochemistry:

RBC - 11.94 M/µL (*6.60 - 12.20 M/µL*)
Calcium - 11.5 mg/dL (*7.6 - 10.4 mg/dL*)
Total Protein - 8.7 g/dL (*4.8 - 8.3 g/dL*)
Albumin - 3.6 g/dL (*2.6 - 4.0 g/dL*)
Globulin - 5.1 g/dL (*2.2 - 4.3 g/dL*)
Albumin: Globulin Ratio - 0.7
Cholesterol - 126 mg/dL (*100 - 300 mg/dL*)

Urine Protein Electrophoresis:

At the time of euthanasia, urine protein electrophoresis (IDEXX Diagnostic Laboratories) was pending. The following day, a large peak in the beta fraction (284.74 mg/dL) that appears relatively narrow supporting a possible monoclonal gammopathy was reported. Urine electrophoretograms are best interpreted in correlation with serum electrophoresis to confirm monoclonal gammopathy.

Urine Protein - 340.6 mg/dL
Albumin (EPH) - 11.24 mg/dL
Alpha Globulin % - 27.59 mg/dL
Beta Globulin - 284.74 mg/dL
Gamma Globulin - 17.03 mg/dL

Postmortem Cytology:

Vertebral foramen mass Touch imprints of the surface of the T11 vertebral canal mass are composed of sheets of markedly pleomorphic neoplastic round cells. Round cells have moderate to large amounts of deep to pale blue cytoplasm with variable nuclear-to-cytoplasmic ratio. These cells typically contain a single, eccentrically marked cellular and nuclear pleomorphism. There are rare atypical mitotic figures.

Microscopic Description:

T11 Vertebra: Replacing and effacing the medullary cavity and multifocally infiltrating and destroying the cortical bone to extend into the vertebral foramen and local paravertebral stroma is a densely cellular, unencapsulated, poorly demarcated, infiltrative mass comprised of closely packed round cells arranged in sheets supported by a fine, fibrovascular stroma. Neoplastic round cells have distinct cell borders, moderate amounts of pale eosinophilic cytoplasm with inconsistent perinuclear clearing (Golgi apparatus), and single nucleus. Nuclei are round, paracentral to eccentric, and have coarse to clumped chromatin and up to one prominent nucleolus. Anisocytosis and anisokaryosis are marked, with up to 6-fold difference in nuclear side, as well as occasional megakaryocytic cells and bi- and multinucleated neoplastic cells. Fifteen mitotic figures are seen in 10 [40x x FN22] HPF. Infrequent individual necrotic neoplastic cells are scattered throughout the tumor. Approximately 40**%** of the vertebral cortical bone is lytic due to tumor infiltration and is multifocally replaced by reactive fibroblasts and a fibrocol-

lagenous stroma. The retained cortical bone is multifocally thinned and there is resorption and remodeling characterized by scalloped surfaces and shelves of woven bone bordered by neoplastic cells and reactive fibroblasts. At the periphery of the tumor and within regions of bone resorption there are minimal hemorrhages.

Contributor's Morphologic Diagnoses:

T11 VERTEBRA, MASS REGION: Malignant plasma cell tumor (multiple myeloma/ plasma cell myeloma) with regional cortical bone, skeletal muscle, and adipose tissue invasion; bone loss, resorption, and remodeling; and myelophthisis [mitotic count = 15 mitotic figures in 10 [40x x FN22] HPF]
SPINAL CORD, T11 REGION (slide not included):

1. Hemorrhages, acute, multifocal to coalescing, moderate
2. Axonal degeneration, multifocal to coalescing (ventral and lateral funiculi), severe with markedly dilated myelin sheaths, multifocal intravacuolar fragmented myelin and macrophages (ellipsoids/ digestion chambers); multifocal swollen axons (spheroids); and marked reactive glial cells [compression myelopathy]

SPLEEN (slide not included):

1. Multifocal to coalescing malignant plasma cell tumors (multiple myeloma/plasma cell myeloma), multifocal with atypia [mitotic count = 11 mitotic figures in 10 [40x x FN22] HPF]
2. Extramedullary hematopoiesis, chronic, multifocal, moderate

Contributor's Comment:

The submitted ferret's presentation of acute non-ambulatory paraparesis and distended urinary bladder with large residual urine volume, along with reported neurolocalization, supported a T3-L3 myelopathy of unclear origin. Potential differentials for this ferret's clinical presentation of acute paresis included metabolic disease (i.e., insulinoma, hyperadrenocorticism, prolonged estrus), neoplasia (i.e., plasma cell tumor (solitary osseous plasmacytoma, multiple myeloma), lymphoma, chordoma, osteoma, osteosarcoma), Aleutian disease, intervertebral disc disease, vertebral congenital malformations, and primary myelitis.[11] Autopsy confirmed a mass originating within the T11 vertebra associated with marked osteolysis and extension into the vertebral canal, as well as extension into the surrounding fibrous and adipose tissue stroma. Compressive myelopathy secondary to tumor growth was confirmed. Consistent with the antemortem abdominal ultrasound, the spleen was severely enlarged with multi-

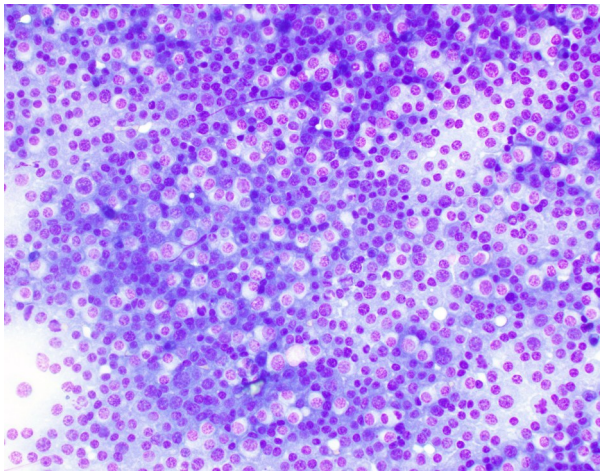

Figure 1-3: Vertebral mass, ferret. A touch impression demonstrates numerous round cells with excentric moderately anisokaryotic nuclei. (*Photo courtesy of*: Schwarzman Animal Medical Center, 510 East 62nd St. New York, NY 10065. http:// www.amcny.org) (Wright-Giemsa 1000X)

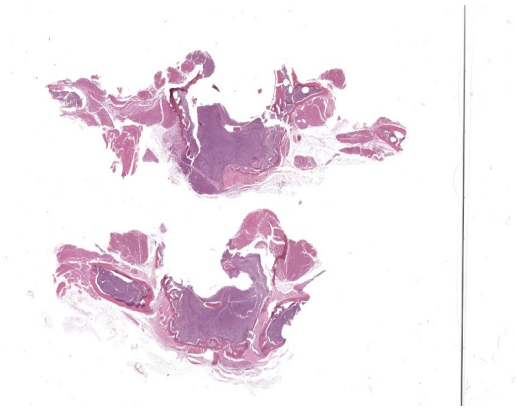

Figure 1-4: Thoracic vertebra, ferret: At subgross magnification, an infiltrative neoplasm effaces the medullary cavity and cortex of the ventral vertebral body, and extends into the underlying epaxial muscle and soft tissue and into the overlying spinal canal. (HE, 10X)

ple white foci and nodules. Microscopic examination confirmed a neoplastic population of plasma cells in both the vertebrae and spleen suggestive of multiple myeloma/ plasma cell myeloma. After gross postmortem examination, findings of the previously submitted urine electrophoresis reported a relatively narrow, large peak in the beta fraction supportive of a possible monoclonal gammopathy. An additional finding in this patient of unclear clinical significance was a single pancreatic neuroendocrine tumor, which was confirmed as an insulinoma with immunohistochemistry for insulin.

Tumors originating from plasma cells include extramedullary plasmacytoma, solitary osseous plasmacytoma, and multiple myeloma (plasma cell myeloma). Plasmacytomas are the most common plasma cell tumors in dogs, and are described frequently in cats and uncommonly in other species.[15,32] Plasmacytomas are typically solitary and are most commonly described in the skin/ subcutis, oral cavity, gastrointestinal tract (particularly colorectal region), but can occur in any organ.[7,9,18,24,30,32,33] Plasmacytomas are typically benign and surgical excision is generally considered curative.[5,7,9,24,32,33] However, infrequent reports of plasmacytomas displaying relatively more aggressive behavior have been described in both dogs and cats.[6,9,32] Cutaneous plasmacytomas over the face can display local tissue invasion, including into the underlying bone.[33] Rare cases of plasmacytoma with associated monoclonal gammopathies are reported in dogs but multiple myeloma should be favored in cases of plasma cell tumor with monoclonal gammopathy.[7,15,32] Solitary osseous plasmacytomas are rare neoplasia reported in people, dogs, and ferrets,[15,25,29] and in humans may represent an early stage of multiple myeloma.[22,25,29] Solitary osseous plasmacytomas represent lytic, locally destructive tumors affecting a single site and not associated with gammopathy,[15,22,25,29] and have been reported in the vertebrae, jaw, carpus, long bones, and ribs of dogs.[25] Multiple myeloma (plasma cell myeloma) is a rare neoplasm of malignant plasma cells arising in the bone marrow or extramedullary sites (i.e., spleen and liver) associated with hyperglobulinemia.[5-8,14-16,20,23,26,29,31-33] Extramedullary site involvement is more common in the cat.[13,29,32,33] The term myeloma-related diseases (MRD) has been adopted in humans and cats, to describe a group of plasma cell or immunoglobulin-secreting B-cell tumors, of which multiple myeloma is one.[1,8,13,14,15,22,32] Multiple myeloma is more commonly reported in dogs and to a lesser extent in cats, including a non-domestic feline.[6,7,13,20,24,26,29,32] Multiple myeloma represents approximately 0.3-1**%** and <1% of all malignancies in dogs and cats, respectively.[1,6,7,14,21,23,26,29,31,34] Cases in other species (horses, cows, pigs, rabbits) are uncommon.[5,7,12,20,23,24,32] Multiple myeloma is more common in middle aged to older animals1,[5,16,22,23,26,29,34]; however, an atypical

presentation in three juvenile dogs have been reported.[22,34] There is no breed or sex predilection in dogs.[31,32] In cats, a male predominance has been reported.[6,14,23,29] In dogs, altered cell cycle protein cyclin C expression may be associated with tumor development.[32]

A common, but not consistent, feature of multiple myeloma is the production of immunoglobulin (Ig) or Ig fragments (paraprotein or M-protein) leading to a gammopathy on electrophoresis, which is most typically monoclonal and less commonly biclonal.[5-8,14,16,21-23,26,29,31-33,36] Light-chain fragments, unattached to heavy chain portions, are filterable though the glomeruli leading to Bence-Jones proteinuria.[6-8,21,22,29,32] Evaluation of densitometric M-protein concentration can be used to evaluate response to therapy.[21,22] Non-secretory myeloma, lacking a gammopathy, is seen in small percentage of cases.[32,33] Other conditions that can be associated with monoclonal gammopathies include chronic infections (i.e., ehrlichiosis and other tick-borne disease, leishmaniasis, chronic pyoderma, and FIP) and other neoplastic processes (i.e., B-CLL, B-cell lymphoma).[7,23,32-33] The most common clinical signs seen with multiple myeloma are non-specific and include pallor, lethargy, listlessness/weakness, inappetence, anorexia, weight loss, and intermittent vomiting.[14,23,26,29] More specific clinical signs depend on distribution of bone lesions and visceral organ involvement, as well as the clinical ramifications of hyperglobulinemia and hypercalcemia. Pain and lameness are common complaints in dogs due to bone lesion(s).[7,8,32,33] With vertebral column involvement, spinal pain, proprioceptive ataxia, paraplegia, and other neurologic manifestations can be seen.[6,29,33,36] Osteolytic lesions are less common in cats.[1,14,19,22,31,32] CBC and biochemical changes include anemia (most commonly non-regenerative, normocytic, normochromic), thrombocytopenia, various leukopenias, hypercalcemia (related to osteolysis and/or PTHrP production), hyperglobulinemia, hypoalbuminemia, hypercholesterolemia, elevated ALP, and azotemia.[6,8,14,16,23,26,29,31-34,36] Circulating neoplastic cells are rarely reported with multiple myeloma.[7,16,23,29,32] Thrombocytopenia, as well as altered platelet function due to paraproteins, can lead to bleeding diathesis.[23,26,32,33] Precipitation of the paraprotein and immunoglobulins (cryoglobulinemia) at cold temperatures can lead to ischemia damage, as well as bleeding tendencies.[7,28] Polyuria and polydipsia can be seen secondary to hypercalcemia, light-chain proteinuria, or amyloidosis.[33] Associated disease manifestations attributed to hyperglobulinemia, paraproteinemia, and biochemical alterations include hyperviscosity syndrome, renal disease (including glomerulonephritis and nephrotic syndrome), light chain deposition disease, extra-tumoral amyloidosis, hypertension, heart failure, immunosuppression, and retinopathy or retinal hemorrhages.[5,7,14,19,23,26,28,29,31,32,36] Myelomatous pleural effusion is a rare clinical manifestation described in people and cats.[1,14] When present,

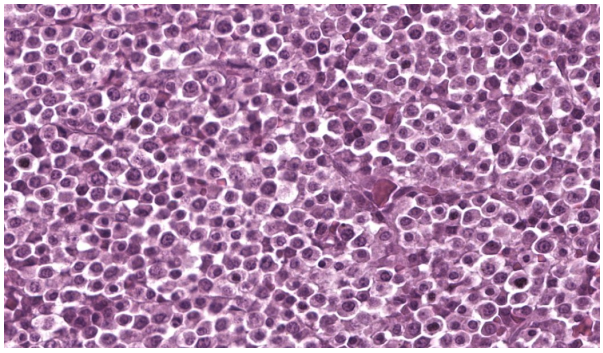

Figure 1-5 Thoracic vertebra, ferret: High magnification of neoplastic cells closely mirrors the cytologic presentation of sheets of round cells with moderate anisokaryosis and excentric nuclei. (HE, 1127X)

osteolytic bone lesions tend to involve areas of active hematopoiesis.[13,29] In small animals, the vertebra (particularly thoracolumbar), femur, pelvis, humerus, skull, and ribs are the most common sites.[6,8,29,34] On imaging, bone lesions are classified most commonly as discrete, "punched out" lytic lesions, typically in multiple bones, with variable sclerotic margins and periosteal reactions.[6,8,16,23,29] Less common imaging patterns include permeative lysis, small lytic foci, homogenous, soft tissue attenuating intramedullary masses, and generalized osteoporosis.[8,29] Pathologic fractures can be seen.[6-8,14] In one case series of bone lesions of computed tomography (CT) in dogs, all the studied dogs had axial skeleton involvement and 69% had concurrent appendicular skeleton lesions.[8]

On gross examination of affected bones, the trabecular bone/medullary cavity are replaced and filled by a soft, fleshy to gelatinous, dark red to grey-pink nodules and masses.[6,29] Histology shows focal or locally extensive solid tumors of densely packed neoplastic plasma cells arranged in sheets, cords, and packets that replace the hematopoietic cells and adipose tissue of the medullary cavity and are supported by a fine fibrous stoma.[6,7,16,29,32] Cortical bone destruction with/or without local soft tissue invasion can be seen.[29] Cellular features of plasma cell differentiation include round cells with moderate to large amounts of amphophilic to basophilic cytoplasm with perinuclear clearing (Golgi apparatus).[7,9,16,18,22,30,32] Nuclei are paracentral to eccentrically placed with clumped chromatin that aggregate in the center or along the nuclear membrane ("clockface" pattern).[7,9,16,18,22,32] Mott cells with prominent cytoplasmic vacuoles (Russel bodies) containing immunoglobulins and may result from altered intracellular protein transport.[18,22,32] Due to differences in stain protocols, these vacuoles can range from semi-clear, to light blue, to pink.[22,32] "Flame cells" are characterized by an outer rim of densely purple or eosinophilic cytoplasm,[32] with light to bright pink projections/blebs or fringe due to accumulation of immunoglobulins.[7,22,23,29] Less well-differentiated tumors display a wider range of cellular and nuclear pleomorphism, variable nuclear-to-cytoplasmic ratio, increased numbers of binucleate and multinucleated cells, and lack of Golgi perinuclear clearing.[29,32] Plasma cell tumors infrequently have intratumoral light chain amyloid (AL-amyloid).[6,7,18,19,22,24,30,32] Erythrophagocytic plasma cell tumors have been described.[3,26] With less differentiated forms, immunohistochemistry (IHC) can be useful to rule-out other round cells tumors. In dogs, MUM1 is the most specific marker for plasma cell tumors.[6,7,9,16,24,26,31-34] Multiple myeloma oncogene 1 (MUM1) is an interferon regulatory transcription factor involved in immunoglobulin light-chain re-arrangement and production of plasma cells.[16,22,24,31,32] Additional tumors that can infrequently be immunoreactive to MUM1 include B-cell lymphoma and anaplastic lymphoma.[24,32] Less consistently plasma cell tumors will stain with λ and κ light chains, Ig heavy chains, CD79a, and CD20.[9,19,22,24,32,33] In one study of canine plasmacytomas, 93.5% of tumors were immunoreactive to MUM1, while only 56.2% and 19.4% of tumors were reactive with CD79a and CD20, respectively.24 In a case series in cats, 32% of MRDs were immunoreactive to CD79+.[19] Methyl green pyronine histochemical stain inconsistently highlight plasma cells.[9]

Traditionally, the presence of multiple osteolytic lesions was strongly suggestive

of multiple myeloma in dogs; however, disease manifestation in cats are different than those reported in both dogs and humans where cats with MRDs typically present with paraproteinemia and have less frequent bone marrow involvement.[1,14,19,22,31,32] In two retrospective studies of MRDs in cats, only a percentage of cats displayed osteolytic lesions (58.3% of studied cats) or bone marrow plasmacytosis (63% of studied cats), and most cats had non-cutaneous, extramedullary plasma cell tumors, typically in the liver and/or spleen in those evaluated for them.[14,23] Thus, extramedullary neoplastic transformation may be more common in cats with MRD than other species,[1, 19, 22, 31] but it is unknown in feline MRD affecting both compartments concurrently arise initially in extramedullary sites with later bone marrow infiltration or extramedullary tumors represent metastases.[14,19] Historically, the diagnostic criteria of multiple myeloma required the presence of two or more of the following features: 1) bone marrow with >20% of plasma cells, 2) osteolytic lesions, 3) serum or urine monoclonal gammopathy, and 4) light-chain proteinuria (Bence-Jones proteinuria).[1,5,7,8,14,16,17,21-24,29,31,33,34,36] Recent studies show the diagnostic criteria of Bence-Jones proteinuria can be fulfilled by documenting free light-chains (fLCs) in urine and/or serum.[8,22,34] Recently, the diagnostic criteria in humans has been updated to add weight to each criteria, as well as incorporate advanced imaging findings, signs of organ-damage, presence of "myeloma-defined events" (hypercalcemia, renal disease, anemia, and bone lysis), and biomarkers of malignancy; and in this updated criteria the threshold of plasmacytosis can be lowered to >10% depending on the clinical picture.[22,23,28] Based on newer information, the threshold for plasmacytosis could be lowered (>10%) in feline cases with visceral organ involvement, presenting hyperglobulinemia or paraproteinemia, and with atypical plasma cell morphologies.[1,14,16,23,29,33] In a retrospective study of multiple myeloma in 16 cats, bone marrow plasmacytosis, ranging from 13-99%, was present in 93.3% of the examined cats, and the majority of these cases (83.3%) had immature and atypical morphologies.[23] The authors advocated for a modified diagnostic criteria in cats to include consideration of plasma cell morphology and visceral organ involvement.[23] In a multi-institutional retrospective study of feline MRDs, of 17 cats with bone marrow involvement 64.7% of cats had plasmacytosis of >10% and 35.3% of cats had bone marrow plasmacytosis ranging from 5-10% with marked cytonuclear atypia.[14] In this series, bone marrow plasmacytosis was rarely seen in cats without splenic or liver involvement (9% of the study population).[14] The authors of this study emphasized the importance of extramedullary involvement and bone marrow cellular atypia as part of the criteria of diagnosis in cats, even when bone marrow plasmacytosis between 5-10%.[14] Current recommendations in cats include at least two of the following: 1) >10% bone marrow plasmacytosis or >5% atypical plasma cells, 2) paraproteinemia, 3) osteolytic lesions, 4) light chain proteinuria, and 5) visceral organ involvement.[14,23,33]

The two most common neoplasms in domestic ferrets arise in the endocrine system (i.e., pancreatic neuroendocrine tumors and adrenal cortical tumors).[2,27,35] The most common hematologic malignan-

cy in ferrets is lymphoma, and spinal lymphoma can present with neurologic dysfunction similar to the submitted case.[11,27,35] Chordomas are the most common neoplastic process in the musculoskeletal system of ferrets, they are low grade malignancies derived from the notochord and can be associated with locally destructive lesions in the vertebral body at any segment of the spinal column and be associated corresponding neurologic symptoms.[27,35] Like the submitted case which had concurrent plasma cell tumors and insulinoma, multiple distinct, synchronous tumors are common in ferrets and up to 20% of ferrets are diagnosed with multiple simultaneous tumors.[27] Like the submitted case, reports of malignant plasma cell tumors, including plasma cell myeloma/multiple myeloma, in ferrets are limited, but in reports hindlimb ataxia and paresis were common clinical complaints and association with vertebral bone tumors was confirmed in multiple cases.[5,17,20,35] Plasma cell tumors have been reported in the bone (most commonly the vertebrae), spleen, liver, lymph node, as well as multicentric disease in ferrets.[2,5,17,20] In addition, a case report of a solitary osseous plasmacytoma associated with secondary vertebral fracture and without gammopathy and extramedullary involvement has been reported in a ferret that presented with non-ambulatory paraparesis, decreased postural reactions, upper motor neuron bladder, and pain.[15] In one case series of malignant plasma cells tumors in six ferrets, clinical signs included hindlimb ataxia and paresis (most common), urinary system signs (either primary or neurologic), and pain.[5] Reported hematologic alterations were variable among the reported ferrets but included anemia, neutrophilia, leukocytopenia, hyperglobulinemia, hyperphosphatemia, hypoglycemia, and hypercalcemia; however, concurrent disease processes may have been a contributing factor in the study cohort (i.e., adrenal disease, inflammatory bowel disease, lymphoma, hemangiosarcoma, insulinoma).[5] In this study population, hyperglobulinemia was most common and monoclonal gammopathy was confirmed in one ferret.[5,35] At the time of diagnosis in this cohort, extramedullary disease was identified in 5/6 cases and dissemination to more than four locations was seen in majority of these.[5] Based on this patient population, malignant plasma cell tumors are aggressive in ferrets and rapidly progressive with a median survival time of 107 days following diagnosis.5 In two single case reports of multiple myeloma/plasma cell myeloma in ferrets, a similar presentation of paraparesis and hind limb paralysis, related to vertebral plasma cells tumors were documented and one of these cases had confirmed extramedullary tumors including in the liver, spleen, lymph nodes, kidney, and thyroid glands.[17,20]

Contributing Institution:

Schwarzman Animal Medical Center, 510 East 62nd St. New York, NY 10065
http://www.amcny.org

JPC Morphologic Diagnosis:

Vertebra, spinal canal, and epaxial musculature: Malignant hematopoietic round cell tumor.

JPC Comment:

Dr. Derron "Tony" Alves, a former Director of the JPC's Veterinary Pathology Service and retired U.S. Army colonel, moderated

this year's 21st conference, providing participants with some fascinating lab animal case selections. This first case sparked an excellent discussion on species-specific pathology in ferrets. Ferrets are notorious for developing a variety of neoplasms, including islet cell tumors, adrenocortical tumors, and lymphoma, all of which should come to the top of the pathologist's mind when approaching ferret cases (especially in the age group of the ferret in this case. This case indeed had a concurrent insulinoma, highlighting the species' tendency toward multiple synchronous neoplasms.

Participants immediately recognized a round cell neoplasm replacing the vertebral marrow cavity. Because participants had only the H&E slide to review prior to conference, and because the neoplastic cells displayed atypia without uniformly classic plasma cell morphology, conference goers agreed that they could not definitively diagnose a plasma cell tumor from the slide alone. As such, the JPC elected to diagnose a malignant hematopietic round cell tumor which would cover both lymphoma (the most common malignancy in this species) as well as myeloma (also a hematopoetic malignancy, but which arises from the bone marrow rather than the lymph nodes or spleen). However, when the full clinical, gross, and laboratory context was revealed, including vertebral osteolysis, splenic involvement, monoclonal gammopathy, classic cytologic findings, and systemic plasma cell proliferation, the case aligned well with multiple myeloma as the final diagnosis. This contrast between what can be stated from the H&E slide alone and what can be concluded from a more comprehensive data set provided an excellent teaching moment on the importance of a full diagnostic work-up in cases such as this.

Participants reviewed the different plasma

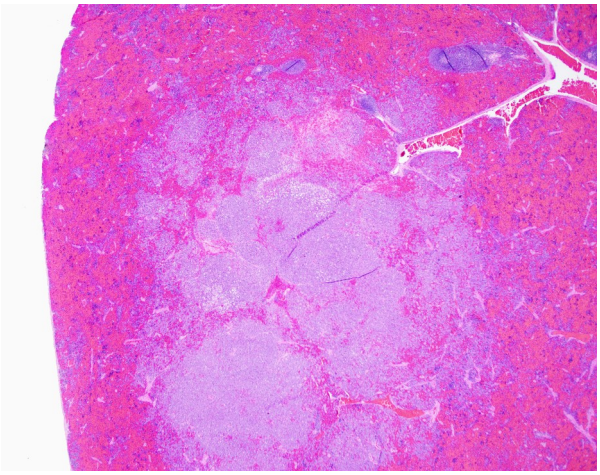

Figure 1-7: Spleen, ferret: Foci of neoplastic plasma cells are scattered throughout the splenic parenchyma. (HE, 100X) : Schwarzman Animal Medical Center, 510 East 62nd St. New York, NY 10065. http://www.amcny.org)

cell tumors, including solitary osseous plasmacytoma. This form serves as a "between" diagnosis that is neither a benign cutaneous plasmacytoma nor a fully systemic multiple myeloma. Osseous plasmacytomas are typically single, isolated bone lesions without gammopathy or visceral involvement, which did not match the full case once ancillary findings were revealed.

The slide also contained several key osseous features, including resting and reversal lines, microfractures, reactive fibrosis, and numerous osteoclasts. All of these are consistent with an aggressive, lytic bone process. Although not present on the H&E slide, the contributor provided some excellent gross and additional histologic images that showed compression myelopathy of the affected area of thoracic spinal cord, serving as a correlation to the pathogenesis of the clinical presentation in this case.

The gross image of marked a markedly enlarged spleen with multifocal, pale tan nodules prompted a strong reminder from Dr. Alves that this pattern should raise suspicion for necrotizing splenitis across species lines. The marked splenic enlargement in this spe-

cies is a common finding in older ferrets and typically associated with extramedullary hematopoesis (noted by the contributor in this case).

The group revisited the clinicopathologic hallmarks of multiple myeloma, which are covered in the contributor's excellent comment.[14,23,33] One participant provided a fantastic reminder that globulins bind calcium in the blood and, when globulins are elevated, this can produce a falsely elevated total calcium on chemistry panels. An ionized calcium is required to confirm true hypercalcemia in such cases. Participants also reviewed other causes of increased gammaglobulins across species lines, such as ehrlichiosis, leishmaniasis, FIP, and chronic pyodermas.

Participants reviewed the different plasma cell tumors, including solitary osseous plasmacytoma. This form serves as a "between" diagnosis that is neither a benign cutaneous plasmacytoma nor a fully systemic multiple myeloma. Osseous plasmacytomas are typically single, isolated bone lesions without gammopathy or visceral involvement, which did not match the full case once ancillary findings were revealed.

The slide also contained several key osseous features, including resting and reversal lines, microfractures, reactive fibrosis, and numerous osteoclasts. All of these are consistent with an aggressive, lytic bone process. Although not present on the H&E slide, the contributor provided some excellent gross and additional histologic images that showed compression myelopathy of the affected area of thoracic spinal cord, serving as a correlation to the pathogenesis of the clinical presentation in this case.

The gross image of marked a markedly enlarged spleen with multifocal, pale tan nodules prompted a strong reminder from Dr. Alves that this pattern should raise suspicion for necrotizing splenitis across species lines. The marked splenic enlargement in this species is a common finding in older ferrets and typically associated with extramedullary hematopoesis (noted by the contributor in this case).

The group revisited the clinicopathologic hallmarks of multiple myeloma, which are covered in the contributor's excellent comment.[14,23,33] One participant provided a fantastic reminder that globulins bind calcium in the blood and, when globulins are elevated, this can produce a falsely elevated total calcium on chemistry panels. An ionized calcium is required to confirm true hypercalcemia in such cases. Participants also reviewed other causes of increased gammaglobulins across species lines, such as ehrlichiosis, leishmaniasis, FIP, and chronic pyodermas.

References:

1. Amalbert T, Canonne AM, and Beguin J. Myelomatous pleural effusion in a cat diagnosed with multiple myeloma. *Journal of Feline Medicine and Surgery Open Reports.* 2023;9 (1):20551169221134094.
2. Avallone G, Forlani A, Tecilla M, et al. Neoplastic diseases in the domestic ferret (*Mustela putorius furos*) in Italy: Classification and tissue distribution of 856 cases (2000-2010). *BMC Veterinary Research*. 2016;12:275.
3. Barger AM, Skowronski MC, and MacNeill AL. Cytologic identification of erythrophagocytic neoplasms in dogs. *Veterinary Clinical Pathology*. 2012;41(4):587-

589.
4. Cantile C and Youssef S. Nervous System. In: Maxie MG, ed. *Jubb, Kennedy and Palmer's Pathology of Domestic Animals*. Vol 1. 6th ed. Philadelphia, PA: Elsevier Saunders; 2016:403.
5. Clagett DO, Johnston MS, and Han S. Malignant plasma cell neoplasia in ferrets: A review of 6 cases. *Journal of Exotic Pet Medicine*. 2017;26:36-46.
6. Craig LE, Dittmer KE, and Thompson KG. Bones and Joints. In: Maxie MG, ed. *Jubb, Kennedy and Palmer's Pathology of Domestic Animals*. Vol 1. 6th ed. Philadelphia, PA: Elsevier Saunders; 2016:123.
7. Durham AC and Boes KM. Bone Marrow, Blood Cells, and the Lymphoid/Lymphatic System. In: Zachary JF and McGavin MD, eds. *Pathologic Basis of Veterinary Disease*. 7th eds. St Louis, MO: Elsevier. 2022;842-843,869.
8. Harris RA, Miller M, Donaghy D, et al. Light chain myeloma and detection of free light chains in serum and urine of dogs and cats. *JVIM*. 2021;35:1031-1040.
9. Hendrick MJ. Mesenchymal Tumors of the Skin and Soft Tissue. In: Mueten DJ, ed. *Tumors in Domestic Animals*. 5th ed. Ames, Iowa: John Wiley and Sons Inc; 2017:171-172.
10. Hoim SE, Fitzgerald E, Mapletoft E, et al. Computed tomographic findings in dogs with multiple myeloma. *Vet Med Sci*. 2023;9:660-669.
11. Ingrao JC, Eschar D, Vince A, et al. Focal Thoracolumbar spinal cord lymphosarcoma in a ferret (*Mustela putorius furo*). *Can Vet J.* 2014;55:667-671.
12. Kameyama M, Ishikawa Y, Shibahara T, et al. Plasma cell myeloma producing IgG, IgM, and IgA immunoglobulins in a cow. *JVDI*. 2003;15:166-169.
13. Kappeli U, Eulenberger U, Nitzl D, et al. Clinical challenge. Multiple myeloma. *Journal of Zoo and Wildlife Medicine*. 2009;40(4):398-401.
14. Lecot L, Desmas-Bazelle I, Benjamin S, et al. Descriptive analysis and prognostic factors in cats with myeloma-related disorders: A multicenter retrospective study of 50 cases. *JVIM.* 2024;38:1693-1705.
15. Liatis T, Gardini A, Marcal VS, et al. Surgical treatment of a vertebral fracture caused by osseous plasmacytoma in a domestic ferret (*Mustela putorius furo*). *Journal of Exotic Pet Medicine*. 2019;29:200-206
16. Marchegiani A, Palumbo Piccionello A, Salvaggio A, et al. What Is Your Diagnosis? J Am Vet Med Assoc. 2016;249(1):47-9
17. Marks AL, Gaschen L, Tully TN, et al. What is your diagnosis? Plasma cell neoplasia. J Am Vet Med Assoc. 2010;237(9):1033-4.
18. Mauldin EA and Peters-Kennedy J. Integumentary System. In: Maxie MG, ed. *Jubb, Kennedy and Palmer's Pathology of Domestic Animals*. Vol 1. 6th ed. Philadelphia, PA: Elsevier Saunders; 2016:735.
19. Mellor PJ, Haugland S, Smith KC, et al. Histopathologic, Immunohistochemical, and Cytologic Analysis of Feline Myeloma-Related Disorders: Further Evidence for Primary Extramedullary Development in the Cat. *Vet Pathol.* 2008;45:159-173.

BK, et al. Solitary osseous plasmacytoma in dogs: 13 cases (2004-2019). *JSAP.* 2021;62:1114-1121.
26. Romanelli P, Recordati C, Rigamonti P, et al. Erythrophagocytic multiple myeloma in a dog. JVDI. 2022;34(4):718-722.
27. Schoemaker NJ. Ferret Oncology: Diseases, Diagnostics, and Therapeutics. *Vet Clin Exot Anim*. 2017;20:183-208.
28. Spyropoulou M, Montanes-Sancho I, Gow AG, et al. Cryoglobulinemia associated with multiple myeloma in dog presenting with epistaxis and skin lesions. *Veterinary Medicine and Science*. 2024;10:e70084.
29. Thompson KG and Dittmer KE. Tumors of Bone. In: Mueten DJ, ed. *Tumors in Domestic Animals*. 5th ed. Ames, Iowa: John Wiley and Sons Inc;2017:412-414.
30. Uzal FA, Plattner BL, and Hostetter JM. Alimentary System. In: Maxie MG, ed. *Jubb, Kennedy and Palmer's Pathology of Domestic Animals*. Vol 2. 6th ed. Philadelphia, PA: Elsevier Saunders;2016:27-28.
31. Valente PCLG, Peleteiro MC, Dias MJ, et al. Multiple myeloma in dogs: Use of the cell block technique as a new diagnostic tool. Vet Clin Pathol. 2024;53(1):93-98.
32. Valli VE, Bienzle D, Meuten DJ, and Linder KE. Tumors of the Hemolymphatic System. In: Mueten DJ, ed. *Tumors in Domestic Animals*. 5th ed. Ames, Iowa: John Wiley and Sons Inc;2017:218-225.
33. Valli VEO, Kiupel M, and Bienzle D. Hematopoietic System. In: Maxie MG, ed. *Jubb, Kennedy and Palmer's Pathology of Domestic Animals*. Vol 3. 6th ed. Philadelphia, PA: Elsevier Saunders;2016:137,226-228.
34. Wachowiak IJ, Moore AR, Avery A, et al. Atypical multiple myeloma in 3 young dogs. *Veterinary Pathology*. 2022;59 (5):787-791.
35. Williams BH and Wyre NR. Neoplasia in Ferrets. *Ferrets, Rabbits, and Rodents*. 2020;92-108.
36. Wyatt S, De Risio L, Driver C, et al. Neurologic signs and MRI findings in 12 dogs with multiple myeloma. *Vet Radiol Ultrasound*. 2019;60:409-415.

CASE II:

Signalment:

Adult male Fischer 344 (F344) rat (*Rattus norvegicus*)

History:

This rat was part of a research study and was exposed to a chemical on 10/20/2014. He was then found dead on 11/28/2024.

Gross Pathology:

Received for autopsy is a 389g, adult, male Fischer 344 rat with a body condition score of 3/5, adequate subcutaneous and visceral fat, and in full rigor mortis. There is mild autolysis. There is multifocal, patchy thin-

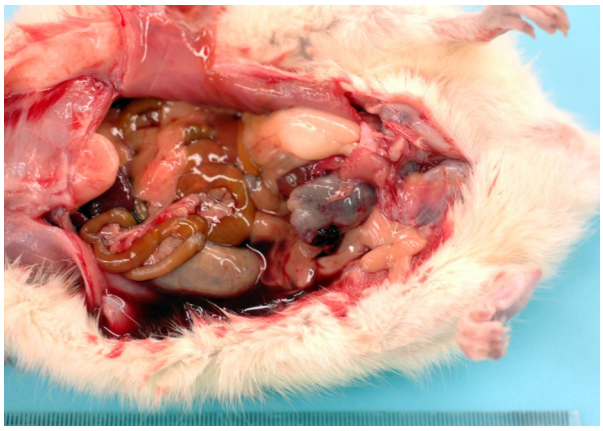

Figure 2-1: Abdominal viscera, rat: The markedly and irregularly distended urinary bladder is ruptured with an adherent blood clot. (*Photo courtesy of:* Comparative Pathology Department at the Institute of Chemical Defense, https://usamricd.health.mil/)

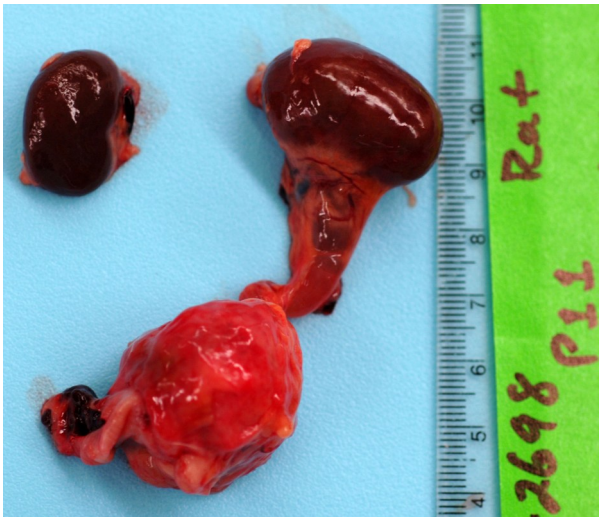

Figure 2-2: Kidneys, ureter, urinary bladder, rat: The left kidney is 3 x 2 x 1.5 cm and the left ureter is 5 mm in diameter (hydronephrosis and hydroureter). The urinary bladder is expanded by a 2.5 cm, round, firm, mass. (*Photo courtesy of:* Comparative Pathology Department at the Institute of Chemical Defense, https://usamricd.health.mil/)

ning of the haircoat along the dorsum with multifocal scabs; a section is taken for histology. The abdominal cavity feels doughy. Upon incising the abdominal cavity, there is approximately 10 mL of serosanguineous fluid in the abdomen (uroperitoneum). The lungs collapse when the diaphragm is cut; they are inflated with 10 mL of 10% NBF. The stomach is full of yellow-gray ingesta. There is scant to moderate amounts of green-brown digesta in the moderately autolyzed small intestines. The cecum is full of dry, green-gray digesta. The distal colon in empty and the proximal colon contains few fecal pellets. The urinary bladder is ruptured with clotted blood adhered to the edges of the rupture. On the dorsal left side of the urinary bladder is a 2.5 cm, round, firm, mass that is pale white and homogenous with central necrosis on cut section. The left kidney is 3 x 2 x 1.5 cm and the left ureter is 5 mm in diameter (hydronephrosis and hydroureter). There are multifocal red-orange, 1-3 mm foci of neoplasia in the right testicle (suspect interstitial cell tumor). All other organs examined appear grossly normal.

Laboratory Results:

Cytologic findings (touch impression of the mass): This fair quality, highly cellular cytologic specimen is composed of a mixture of rafts of tightly adherent polygonal epithelial cells, smaller clusters of epithelial cells, and occasional individualized epithelial cells. There is marked anisocytosis and anisokaryosis with cells measuring 3-12 erythrocytes in diameter and nuclei measuring 2-8 erythrocytes in diameter. Cells have abundant light blue, occasionally vacuolated cytoplasm. Nuclei have reticulated chromatin and occasional prominent nucleoli. Many cells exhibit high nuclear:cytoplasm ratio. There are occasional bi- and multi-nucleated cells. This is on a background of abundant cellular debris, viable and degenerate neutrophils, cocci and coccobacilli bacteria, macrophages, stain precipitate, and naked and streaming nuclei.

Microscopic Description:

Urinary bladder: Arising from urothelium, infiltrating and expanding the lamina propria, and surrounding the ureter is a non-

Figure 2-3: Urinary bladder and kidney, rat A section of urinary bladder with a large transmural neoplasm (left) and a concave section of hydronephrotic kidney are submitted for examination. (HE, 9X)

encapsulated, well demarcated, moderately cellular neoplasm composed of polygonal cells arranged in nests on a fibrovascular stroma. Each neoplastic cell has indistinct cell borders, a moderate amount of pale basophilic cytoplasm, with a single misshapen nucleus with finely stippled chromatin and 1 -3 distinct nucleoli. Anisocytosis and anisokaryosis are moderate. There are 2 mitotic figures per 2.37mm^2. The neoplastic nests are often separated by a robust scirrhous response. Multifocally the neoplastic cells are replaced by eosinophilic, amorphous material (necrosis).

Prostate gland: Multifocally, prostatic glands are filled with cellular debris and degenerate neutrophils.

Kidney: There is severe dilation of the renal pelvis with marked thinning of the renal medulla and cortex.

Contributor's Morphologic Diagnosis:

Urinary bladder: Urothelial cell carcinoma, *Rattus norvegicus*.

Kidney: Hydronephrosis, severe.

Prostate gland: Prostatitis, neutrophilic, mild.

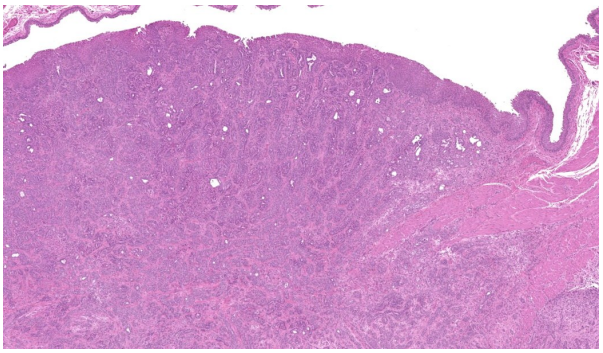

Figure 2-4: Urinary bladder, rat. A transmural neoplasm extends downward from the ulcerated epithelium and effaces the wall of the bladder. (HE, 58X)

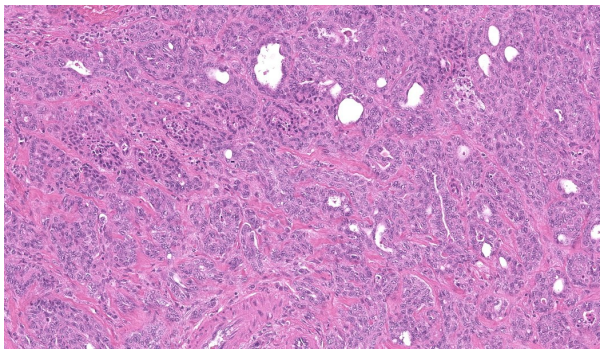

Figure 2-5: Urinary bladder, rat. Neoplastic epithelial cells are arranged in trabeculae and occasional glands on a dense fibrous stroma. (HE, 278X)

Contributor's Comment:

The cause of death in this animal is a ruptured urinary bladder secondary to outflow obstruction from a urinary tumor. The tumor observed both grossly and microscopically is consistent with a urothelial cell carcinoma of the urinary bladder epithelium. Spontaneous urothelial cell carcinomas of the urinary bladder are rare in rats. Although they may be locally invasive, they rarely metastasize. In this case, both the size of the tumor and the strong scirrhous response contributed to the outflow tract obstruction (and therefore an inability to urinate) and urinary inflow tract obstruction from the left kidney (resulting in unilateral hydronephrosis and hydroureter).

This case lacks Melamed-Wolinksi (MW) bodies, which are not listed as a feature in rats[(1)]. MW bodies were first described in 1961 by Melamed and Wolinska while studying 500 urine cytology specimens[(2)] and are defined as single to many round red-or green cytoplasmic inclusions seen in degenerated urothelial cells; however, MW bodies are not always round.[(3)] Cells with MW bodies when noted in body fluids (e.g., pleural fluid, ascitic fluid) signify urothelial origin and suggest metastasis. Recent studies suggest MW bodies are enlarged lysosomes occur-

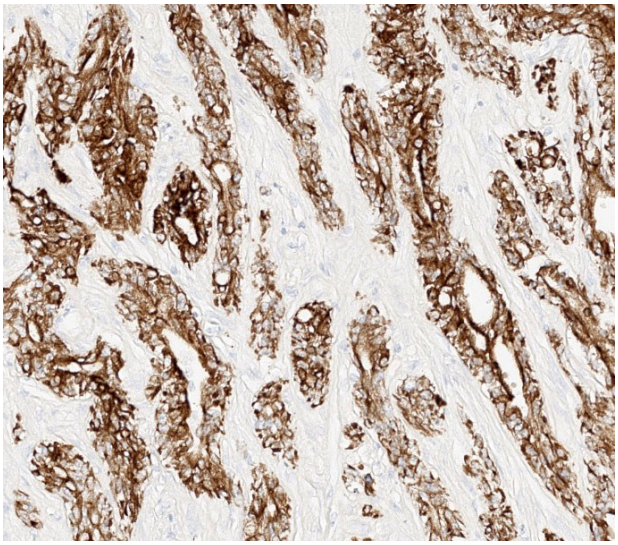

Figure 2-6: Urinary bladder, rat: Neoplastic cells demonstrate strong cytoplasmic immunoreactivity for cytokeratin (anti-AE1/AE3, 400X)

ring in degenerating urothelial cells.[2]

In addition to the urinary bladder tumor, this case provides a great example of what happens upstream of the urinary bladder when it is blocked. At www.medicinepoems.com, there is an 8-stanza ode to hydronephrosis. The second stanza reads as follows:

Hydronephrosis, the name it bears in pain,

A flood within the kidney's fragile frame,

Where once smooth flow of life's essential stream,

Is halted now, a blocked and troubled dream.

Contributing Institution:

Comparative Pathology Department at the Institute of Chemical Defense

https://usamricd.health.mil/

JPC Morphologic Diagnosis:

1. Urinary bladder: Urothelial cell carcinoma.
2. Kidney: Hydronephrosis, chronic, diffuse, severe.

JPC Comment:

First of all, if you missed the poem above, go read it now. It is a blessing for the WSC to have been graced by an ode to hydronephrosis such as this.

This case generated rich discussion on the importance of strain-specific background pathology. As is true for most laboratory rat strains, the Fischer 344s come with genetic baggage. They are predisposed to large granular lymphocytic leukemia, testicular mesothelioma (typically the epithelioid variant), and testicular interstitial cell tumors, the last of which can induce hypercalcemia in this strain. While none of these were primary considerations in this case, the reminder served as a useful anchor for approaching pathology in this particular strain.

Differential diagnoses for this urinary bladder mass included urothelial cell carcinoma, prostatic carcinoma, and renal carcinoma, with the latter two included largely to ensure that metastatic or locally invasive disease was not being overlooked. The histologic architecture of an infiltrative epithelial neo-

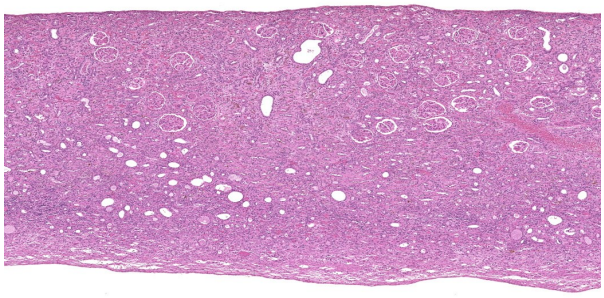

Figure 2-7: Kidney, rat. The urinary pelvis is markedly dilated, resulting in a concave appearance to the kidney (hydronephrosis). The medulla (bottom), and to the lesser extent, cortex (top) are compressed with marked loss of nephrons, occasional ectasia of remnant tubules and fibrosis. (HE, 86X)

plasm seemingly arising from the bladder wall favored a urothelial origin, but immunohistochemistry provided an additional layer of information. The neoplastic cells were diffusely immunoreactive for CK7, a cytokeratin expressed in most primary urinary bladder carcinomas.[4] They were negative for GATA3, a transcription factor involved in urothelial differentiation, which may suggest prostatic carcinoma instead.[5] However, Dr. Alves noted that GATA3 is most reliable in well-differentiated urothelial carcinomas, and its absence here is also consistent with less well-differentiated UCCs, as in this case.[5] The tumor was also negative for PAX8, a marker of renal tubular epithelium, which helped exclude renal carcinoma.[2] Uroplakin, a highly specific marker for urothelial cell carcinoma, unfortunately did not work in this case.[7] Participants also discussed the glandular differentiation present within the tumor, which can be seen in both urothelial cell and prostatic carcinomas. In humans, glandular differentiation in urothelial carcinoma is associated with invasion and poorer differentiation.[8] While extrapolating across species is something to be avoided, the same pattern was evident here.

One of the most instructive aspects of this case was the hydronephrosis, which was beautifully captured on the H&E slide. Dr. Alves emphasized not to overlook this lesion: the upstream consequences of urinary outflow obstruction (pelvic dilation, cortical and medullary thinning, tubular atrophy) were classic! The obstruction in this rat was likely caused by the combination of the tumor's size and its pronounced desmoplastic response, which occluded the bladder outlet.

References:

1. Ayra P, Khalbuss WE, Monaco SE, Pantanowitz L. Melamed-Wolinska bodies. *Diagn Cytopathol*. 2012;40:150-1.

2. Barr ML, Jilaveanu LB, Camp RL, Adeniran AJ, Kluger HM, Shuch B. PAX-8 expression in renal tumours and distant sites: a useful marker of primary and metastatic renal cell carcinoma?. *J Clin Pathol*. 2015;68(1):12-17.

3. Frazier KS, Seely JC, Hard GC, et al. Proliferative and Nonproliferative Lesions of the Rat and Mouse Urinary System. *Toxicologic Pathology*. 2012;40(4_suppl):14S-86S.

4. Jiang J, Ulbright TM, Younger C, et al. Cytokeratin 7 and cytokeratin 20 in primary urinary bladder carcinoma and matched lymph node metastasis. *Arch Pathol Lab Med*. 2001;125(7):921-923.

6. Liang Y, Heitzman J, Kamat AM, Dinney CP, Czerniak B, Guo CC. Differential expression of GATA-3 in urothelial carcinoma variants. *Hum Pathol*. 2014;45(7):1466-1472.

7. Rashidi B, Tongson-Ignacio JE. Melamed-Wolinska bodies in urine cytology an interesting aggregate in a degenerated urothelial cell. *Diagn Cytopathol*. 2011;39:117.

8. Tian W, Guner G, Miyamoto H, et al. Utility of uroplakin II expression as a marker of urothelial carcinoma. *Hum Pathol*. 2015;46(1):58-64.

9. Zhao G, Wang C, Tang Y, et al. Glandular differentiation in pT1 urothelial carcinoma of bladder predicts poor prognosis. *Sci Rep*. 2019;9(1):5323.

CASE III:

Signalment:

14-month-old female intact common mar

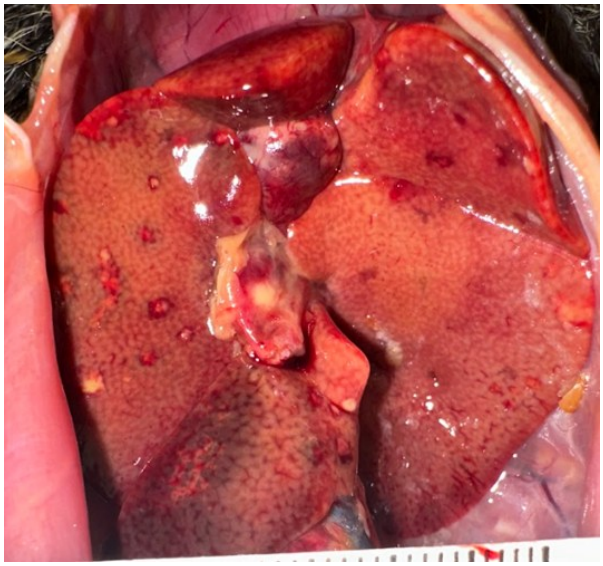

Figure 3-1: Liver, marmoset: The liver is diffusely yellow orange and contains distributed throughout all liver lobes were randomly dispersed yellow-white and red rimmed, ~0.5 cm diameter, foci that extended into the parenchyma on cut section. (*Photo courtesy of:* Laboratory of Comparative Pathology; Memorial Sloan Kettering Cancer Center, https://www.mskcc.org/research/ski/core-facilities/comparative-medicine-pathology-0)

moset (*Callithrix jacchus*)

History:

This marmoset was presented with a sudden onset of lethargy and anorexia. The marmoset died approximately 18 hours post clinical evaluation and initiation of medical treatment.

Gross Pathology:

Examined was a female marmoset in fair nutritional condition (2.5/5) with mild post-mortem autolysis. Distributed throughout all liver lobes were yellow-white and red rimmed, ~0.5 cm diameter, randomly dispersed foci that extended into the parenchyma on cut section. The parenchyma was diffusely orange with an enhanced reticular pattern (Fig. 1). The lungs were diffusely bright red and atelectatic. Sections from all pulmonary lobes floated in formalin. There was marked diffuse gas dilation of the stomach. All segments of the small intestine were moderately to markedly distended by air and contained small amounts of digesta. The pancreatic lymph node adjacent to the duodenum was approximately 3x the size of normal. The cecum and colon had multifocal white to pale tan, circular areas of serosal discoloration. There were formed feces in the colon.

Laboratory Results:

Bacterial species identification confirmed by MALDI-TOF mass spectrometry:

Liver, aerobic culture: 3+ *P. aeruginosa* and <1+ *K. pneumoniae*

Liver, anaerobic culture: *Clostridium barattii* on thiglycolate

Lung, aerobic culture: 3+ *P. aeruginosa*, 1+ *K. pneumonia* and *Ligilactobacillus rauteri*

Cecum, aerobic culture: 3+ Mixed bacterial sps. included: *Pseudomonas aeruginosa*, *Proteus mirabilis*, *Klebsiella pneumonia, Citrobacter freundii* and *Citrobacter farmer*

K. pneumonia string test: negative

P. aeruginosa ISH of liver: bacteria strongly positive, located diffusely within sinusoids and concentrated around vessels (Fig. 3 & 4).

Gram stain: Gram-negative rod-shaped bacteria associated with areas of inflammation and necrosis in the liver and gallbladder and presence of Gram-negative bacteria in circulation

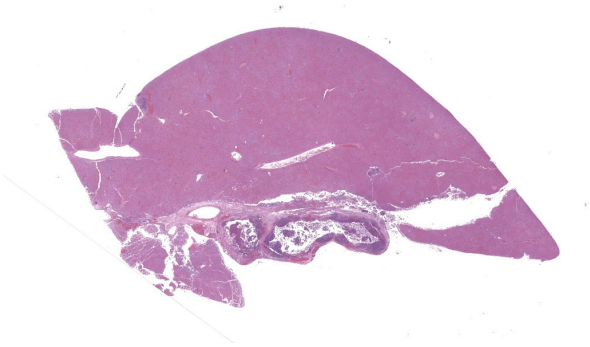

Figure 3-2: Liver and gallbladder, marmoset: A section of liver and gallbladder are submitted for examination. The wall of the gallbladder is effaced by necrosis and inflammation. (HE, 10X).

in the glomeruli and pulmonary vasculature

Microscopic Description:

Gallbladder and liver: The gallbladder and adjacent portal tracts are effaced by multifocal to coalescing areas of coagulative and lytic necrosis admixed with foci of suppurative inflammation. The gallbladder is transmurally severely expanded by numerous neutrophils, scattered lymphocytes and histiocytes, abundant polymerized fibrin, necrotic debris eosinophilic proteinaceous fluid (edema), extravasated red blood cells (hemorrhage), and mats of extracellular rod-shaped bacteria (bacilli). Multifocally, blood vessels in the gallbladder are distorted by endothelial and/or mural necrosis and innumerable bacilli. Some vessels are partially occluded by fibrin and bacterial thrombi. Remaining intact vessels are congested. There is marked loss of gallbladder epithelium characterized by hypereosinophilia and loss of nuclear detail (necrosis), occasionally seen sloughing into the lumen admixed with neutrophils, fibrin, and red blood cells. Throughout the liver, bile ducts and portal vasculature undergo similar changes of varying severity (Fig 2). Bacilli are located extracellularly within portal areas and within sinusoids or intracellularly within macrophages. There are moderate, acute, multifocal loss of hepatocellular detail admixed with areas of fragmented chromatin and karyolytic debris (coagulative and lytic necrosis). Remaining hepatocytes are mildly to moderately swollen by small to medium-sized, round, clear, cytoplasmic vacuoles.

Contributor's Morphologic Diagnosis:

1. Gallbladder: Severe, acute, multifocal to coalescing, necrotizing and suppurative, transmural cholecystitis with hemorrhages, congestion, polymerized fibrin, edema, and intralesional bacilli
2. Vasculature, gallbladder and liver: Marked, acute, multifocal endothelial necrosis with mural bacterial colonization, bacteremia, and fibrin thrombi
3. Liver: Severe, acute, multifocal, necrotizing and suppurative cholangiohepatitis with multifocal hemorrhages, acute random hepatic necrosis, and intralesional bacilli
4. Liver: Mild to moderate, multifocal, microvesicular steatosis

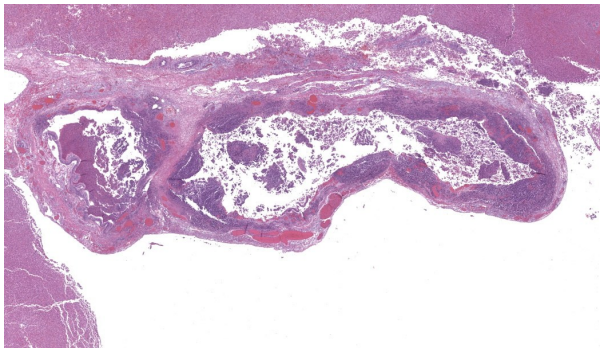

Figure 3-3: Gallbladder, marmoset: The wall of the gallbladder is transmurally necrotic with infiltration of innumerable neutrophils and hemorrhage. The lumen contains abundant cellular debris. (HE, 27X).

Contributor's Comment:

The cause of death of this marmoset was due systemic bacterial infection that likely originated in the upper small intestine, resulting in an ascending biliary tree infection and translocation into the blood supply. Intravascular bacteria were identified in the heart, lung, kidneys, liver, gallbladder, duodenum, mesentery, cecum, and adrenal glands. Necrotic foci and hemorrhage were identified in the stomach, cecum, and mid-colon; these lesions lacked leukocytic cell infiltrates and were therefore considered peracute and secondary to sepsis/toxemia. Bacterial translocation across these lesions resulting in bacteremia cannot be ruled out.

In the case presented here, both *P. aeruginosa* and *K. pneumoniae* were isolated from the liver and lung. Given the gross and microscopic findings of acute hepatic necrosis and strong positive *P. aeruginosa* ISH, *P. aeruginosa* was determined to be the most likely primary pathogen. *K. pneumoniae* infections in non-human primates tend to form abscesses, which is not a feature of this infection.[12] Additionally, we did not observe clear halos surrounding the bacilli when associated with leukocytes, which is a microscopic feature when dealing with hypervirulent *K. pneumoniae* outbreaks in NHPs. This marmoset also had a mild to moderate chronic lymphoplasmacytic enteritis with the duodenum most affected. Microbiome studies comparing healthy and sick captive marmosets affected by IBD or duodenal strictures/dilatation syndrome from different facilities demonstrated significant alterations in the diversity and shifts in their bacterial flora in the small intestine in sick marmosets.[19,20] We cannot rule out the possibility that IBD may have contributed to alterations in the normal bacterial flora and facilitating the translocation of pathogenic bacteria in this case.

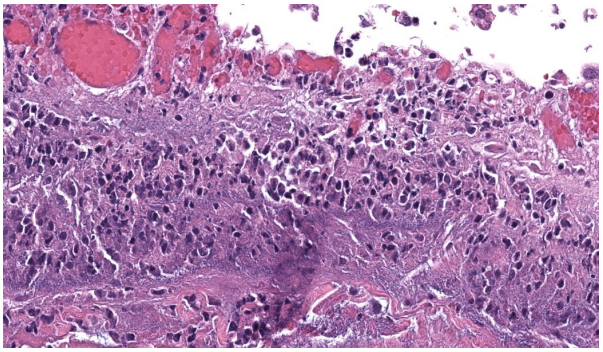

Figure 3-4: Gallbladder, marmoset: Within the necrotic wall, there are innumerable bacilli. (HE,696X).

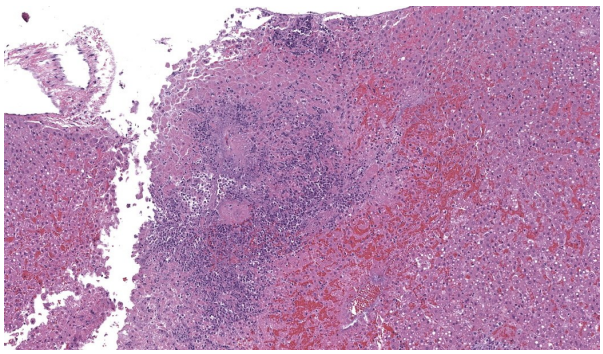

Figure 3-5: Liver, marmoset: Areas of necrosis and hemorrhage, with bacilli, are scattered within the hepatic parenchyma. (HE, 273X).

Pseudomonas species are motile, gram negative, bacillary, opportunistic pathogens of humans, animals, and plants. *P. aeruginosa* is associated with various diseases in veterinary species that include, but are not limited to, the following: septicemia in newly-hatched chickens and late stage embryos;[11] mastitis in cattle, sheep, and goats;[5,14] fleece rot in sheep;[6] pyoderma, otitis externa, and ulcerative keratitis in in dogs and cats;[8,17,18] hemorrhagic pneumonia in mink;[1] metritis in mares;[7] mouth rot (necrotic stomatitis) in snakes;[4] otitis media, pneumonia, septicemia enteritis, and sudden death chinchillas;[9] and wound infections in many species. In hu-

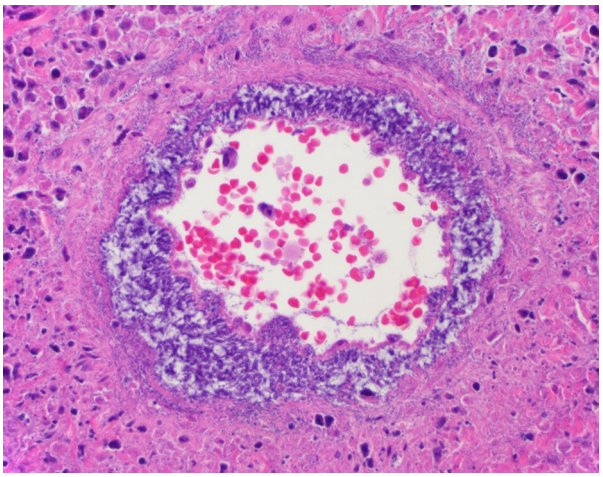

Figure 3-6: Liver, marmoset: Hepatic vessel surrounded by numerous bacilli indicates sepsis. (HE, 400X). (*Photo courtesy of:* Laboratory of Comparative Pathology; Memorial Sloan Kettering Cancer Center, https://www.mskcc.org/research/ski/core-facilities/comparative-medicine-pathology-0)

mans, this bacterium is often associated with infections in critically ill and immunocompromised patients. Over many years, *P. aeruginosa* isolates from hospital-acquired infections in humans have become increasingly antimicrobial resistant, and treatment options are limited.[2]

P. aeruginosa contains an array of virulence factors, allowing it to cause a wide variety of clinical diseases.[10] The outer membrane contains lipopolysaccharide, which modulates adherence to epithelial cells, evasion of phagocytosis, and activation of host immune response leading to dysregulated cytokine production. Biofilm formation is modulated by production of alginate and other exopolysaccharides. The flagellum allows for bacterial dispersion through aqueous and low-viscosity environments, relying on chemotaxis to swim toward epithelial cells. Pili are primarily used for epithelial cell adherence. A type III secretion system injects several cytotoxins and exotoxins that cause rapid host cell death. Several extracellular proteolytic enzymes, such as alkaline proteases and elastases, can cause significant host tissue damage and subsequent invasion. Because iron is required for bacterial growth, the bacteria has siderophores to scavenge this nutrient.[10,22]

P. aeruginosa has been isolated from squirrel monkeys with meningitis, pododermatitis and cellulitis, and abscesses; an African green monkey with pneumonia and myocarditis; and from a chimpanzee with suppurative nephritis.[21] Though *P. aeruginosa* is rarely a primary pathogen in marmosets a recent case series reported necrosuppurative cholangiohepatitis and necrotizing typhlitis in 7 indoor housed marmosets common.[16] Infection was attributed to *Pseudomonas* contamination of the water supply. Though *P. aeruginosa* was frequently isolated from lesions in these cases, a subset of lesions recovered both *E. coli* and *P. aeruginosa.*[16]

Contributing Institution:

Laboratory of Comparative Pathology; Memorial Sloan Kettering Cancer Center, Weill Cornell Medicine, Hospital for Special Surgery, and The Rockefeller University
417 E. 68th St., ZRC-940
New York, NY 10065
https://www.mskcc.org/research/ski/core-facilities/comparative-medicine-pathology-0

JPC Morphologic Diagnosis:

1. Gallbladder: Cholecystitis, necrosuppurative, acute, diffuse, severe, with vasculitis and innumerable bacilli.
2. Liver: Cholangiohepatitis, necrosuppurative, acute, multifocal to coalescing, severe, with portal vein thrombi, random hepatocellular necrosis, and

innumerable bacilli.

JPC Comment:

This case, along with the outstanding contributor comment, provided an excellent opportunity to discuss necrotizing hepatitis in marmosets. Dr. Alves emphasized that necrotizing hepatitis in New World primates should immediately bring alphaherpesviruses to mind, including human herpes simplex virus (human alphaherpesvirus-1), macacine herpesvirus 1 (Herpes B), and saimariine herpesvirus 1 (formely known as *Herpesvirus tamarinus* or Herpes T).[13] Other major differentials to consider include lymphocytic choriomeningitis virus (LCMV), and a wide array of "hot gram-negative bacteria" such as *Francisella tularensis*, *Pseudomonas aeruginosa*, and other fulminant septicemic organisms.[13] To foot-stomp this point, participants received a firm reminder to know their alphaherpesviruses, as these agents remain among the most devastating and diagnostically urgent pathogens in Old and New World primates.[13]

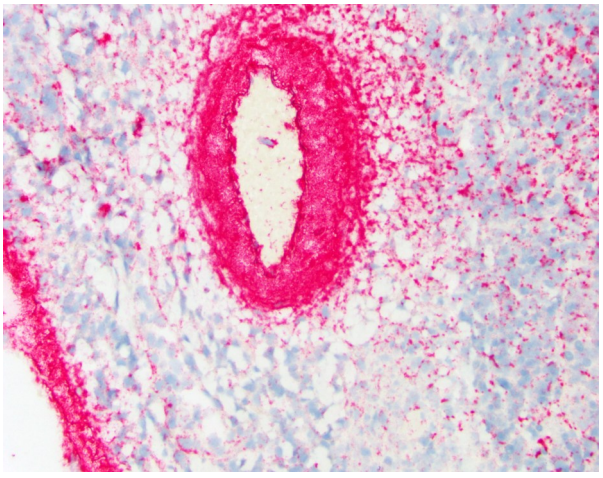

Figure 3-7: Liver, marmoset: Bacilli within the perivascular areas in the liver are positive on ISH for *P. aeruginosa*. (ISH, 400X). (*Photo courtesy of:* Laboratory of Comparative Pathology; Memorial Sloan Kettering Cancer Center, https://www.mskcc.org/research/ski/core-facilities/comparative-medicine-pathology-0)

The hepatic necrosis in this case was acute, and participants noted that cholestasis, which is generally considered a lesion of chronicity, was absent. The lack of viral inclusions also argued against many of the viral pathogens on the differential list. However, Dr. Alves cautioned against prematurely dismissing viruses simply because bacteria are abundant; many viral infections create the perfect environment for secondary bacterial invasion, and the presence of bacteria does not automatically identify the primary pathogen.

In this case, however, the evidence strongly supported *Pseudomonas aeruginosa* as the primary agent, with *Klebsiella pneumoniae* acting as a secondary invader. The bacteria are gram-negative and argyrophilic, and both were cultured from affected tissues. *Klebsiella pneumoniae* infections often produce overt abscessation, "turkey egg" kidneys, and acute renal tubular necrosis.[15] The absence of these lesions further supported the role of *Klebsiella pneumoniae* as a secondary pathogen, although it is more than capable of causing disease on its own.[15]

Participants discussed the most likely pathogenesis of infection as having ascended from the gastrointestinal tract, traveled up the common bile duct, and seeded the gallbladder and liver, producing the necrotizing cholangiohepatitis observed. This concurs with the contributor's proposed cause of death. The ascending route is well-documented in marmosets, particularly in the context of intestinal dysbiosis or chronic enteritis, and is a common route of infection for many enteric gram-negative bacterial pathogens.

Dr. Alves concluded the discussion with a concise review of the pathogenesis of

gram-negative septicemia, emphasizing how rapidly this cascade can overwhelm animals. Circulating endotoxin (LPS) first binds to LPS-binding protein. This complex then engages CD14 on leukocytes. After dissociation of the binding protein, the CD14–LPS complex binds to TLR4, triggering a MyD88-dependent signaling cascade that drives NF-κB and interferon activation.[3] The result is widespread macrophage stimulation with release of cytokines and nitric oxide, followed by endothelial activation and the induction of tissue factor. Tissue factor stimulates the extrinsic coagulation cascade. Once the coagulation cascade is initiated, endothelial injury accelerates, leading to consumptive coagulopathy and, ultimately, the risk of disseminated intravascular coagulation.[3] This mechanistic walkthrough tied together the hepatic necrosis, vascular injury, and multiorgan involvement seen in the case, reinforcing why gram-negative septicemia remains such a devastating process.

References:

1. Bai J, Wang X, Zhang Z, et al. Overview of Mink Immunity and Resistance to *Pseudomonas aeruginosa*. *Vet Med Int*. 2023;(1):6158844.
2. Bassetti M, Vena A, Croxatto A, et al. How to manage *Pseudomonas aeruginosa* infections. *Drugs in context*. 2018;7.
3. Bochud PY, Calandra T. Pathogenesis of sepsis: new concepts and implications for future treatment. *BMJ*. 2003;326 (7383):262-266.
4. Ciobotaru E, Tudor L, Constantinescu CM, et al. *Pseudomonas spp*. induced lesions in non-venomous snakes. *J Comp Path.* 2009;141(4):283.
5. Dapgh AN, Hakim HS. Abouelhag HA, et al. Detection of virulence and multi-drug resistance operons in *Pseudomonas aeruginosa* isolated from Egyptian Baladi sheep and goat. *Vet World*. 2019:12(10):1524.
6. Denmann S, Tellam R, Vuocolo T, et al. Fleece rot and dermatophilosis (lumpy wool) in sheep: opportunities and challenges for new vaccines. *Anim Prod Sci*. 2021;62(4); 301-320.
7. Ferrer MS, & Palomares R. Aerobic uterine isolates and antimicrobial susceptibility in mares with post-partum metritis. *EVJ.* 2018;50(2):202-207.
8. Hillier A, Alcorn JR, Cole LK, et al. Pyoderma caused by *Pseudomonas aeruginosa* infection in dogs: 20 cases. *Vet Derm.* 2006;17(6);432-439.
9. Hirakawa Y, Sasaki H, Kawamoto E, et al. Prevalence and analysis of *Pseudomonas aeruginosa* in chinchillas. *BMC Vet Res*. 2010;6:1-10.
10. Jurado-Martín I, Sainz-Mejías M, & McClean S. *Pseudomonas aeruginosa*: an audacious pathogen with an adaptable arsenal of virulence factors. *Int J Mol Sci.* 2021;22(6);3128.
11. Kebede F. *Pseudomonas* infection in chickens. *J Vet Med Anim Health*. 2010;2(4):55-58.
12. Keesler RI, Colagross-Schouten A, Reader JR. Clinical and pathologic features of spontaneous *Klebsiella pneumoniae* infection in 9 rhesus macaques (*Macaca mulatta*). *Comp Med.* 2020;70 (2):183-9.
13. Mätz-Rensing K, Bleyer M. Viral Diseases of Common Marmosets. *The Common Marmoset in Captivity and Biomedical Research*. 2019;251-264.

14. Park H, Hong M, Hwang S, et al. Characterisation of *Pseudomonas aeruginosa* related to bovine mastitis. *Acta Vet Hung*. 2014;62(1):1-12.

15. Pisharath HR, Cooper TK, Brice AK, et al. Septicemia and peritonitis in a colony of common marmosets (Callithrix jacchus) secondary to Klebsiella pneumoniae infection. *Contemp Top Lab Anim Sci*. 2005;44(1):35-37.

16. Powers SJ, Castell N, Vistein R, et al. Bacterial Cholecystitis and Cholangiohepatitis in Common Marmosets (*Callithrix jacchus*). *Comp Med.* 2023;73 (2):173-180.

17. Pye C. *Pseudomonas* otitis externa in dogs. *CVJ*. 2018;59(11):1231.

18. Santos TM, Ledbetter RC, Caixeta LS, et al. Isolation and characterization of two bacteriophages with strong in vitro antimicrobial activity against *Pseudomonas aeruginosa* isolated from dogs with ocular infections. *Am J Vet Res*. 2011;72 (8):1079-1086.

19. Sheh A, Artim SC, Burns MA, et al. Alterations in common marmoset gut microbiome associated with duodenal strictures. *Sci Rep*. 2022;12(1):5277.

20. Sheh A, Artim SC, Burns MA, et al. Analysis of gut microbiome profiles in common marmosets (*Callithrix jacchus*) in health and intestinal disease. *Sci Rep*. 2022;12(1):4430.

21. Simmons J, Gibson S. Bacterial and mycotic diseases of nonhuman primates. *Nonhuman Primates in Biomedical Research*. 2012:105-72.

22. Rocha AJ, Barsottini MRDO, Rocha RR, et al. *Pseudomonas aeruginosa*: virulence factors and antibiotic resistance genes. *Brazi Arch Biol Techn*. 2019;62, e19180503.

CASE IV:

Signalment:

19 year old, female, African green monkey (*Chlorocebus aethiops sabaeus*).

History:

A 19-year-old, multiparous, fourth-generation colony-bred female African green monkey (*Chlorocebus aethiops sabaeus*) developed a swelling in the lateral aspect of the right thigh region over the course of 5 years. The animal was maintained exclusively for breeding and was not involved in any experimental procedures.

While housed in an outdoor breeding group, the monkey was observed by caretakers to be limping and unable to bear weight on her right hind limb. Upon closer inspection, the lateral thigh region appeared swollen and bruised.

The monkey was treated with multiple doses of nonsteroidal anti-inflammatory drugs and dexamethasone with only partial regression of the swelling. On palpation, the lateral thigh was firm and warm, with no additional abnormalities noted on physical examination.

Gross Pathology:

On postmortem examination, the carcass weighed 3.83 kg and had a body condition of 2 out of 5. The swollen area on the right pelvic limb exhibited mild alopecia and crusting.

Postmortem radiographs showed an extensive, multilocular radiopaque mass within

Figure 4-1: Hindlimb, African green monkey: A multilocular radiopaque mass is present within soft tissues surrounding the latero-caudal aspect of the right hip and stifle. (*Photo courtesy of*: Ross University School Of Veterinary Medicine, https://veterinary.rossu.edu/research/pathology-training-program)

soft tissues surrounding the latero-caudal aspect of the right hip and stifle, extending from the level of the greater trochanter to approximately 10 cm distal to the tibiofemoral joint. The mass did not invade long bones.

Dissection revealed a multilobulated, non-encapsulated, crepitant, yellow to red mass measuring 11 × 5 × 4 cm, infiltrating and replacing the subcutaneous tissue and skeletal muscles of the right thigh.

The mass contained numerous hard, white spicules, suggesting mineralization. The periosteum of the right femur was focally and extensively irregular. No gross pathological alterations were observed in the internal organs.

Laboratory Results:

Laboratory data was not available for this case.

Microscopic Description:

The affected skeletal muscle and subcutis were infiltrated and expanded by abundant, irregular, globoid amphophilic to basophilic material, consistent with mineralization. This mineralized material was surrounded by extensive fibrous connective tissue proliferation (fibrosis), admixed with numerous macrophages, lymphocytes, and fewer multinucleated giant cells containing phagocytosed mineral material. Scattered throughout the mass, rare foci of osteoid formation were observed, characterized by a low number of empty lacunae and necrotic osteoid undergo-

Figure 4-2: Hindlimb, African green monkey: A multilobulated, non-encapsulated, crepitant, yellow to red mass measuring 11 × 5 × 4 cm, infiltrating and replaces the subcutaneous tissue and skeletal muscles of the right thigh. (*Photo courtesy of*: Ross University School Of Veterinary Medicine, https://veterinary.rossu.edu/research/pathology-training-program)

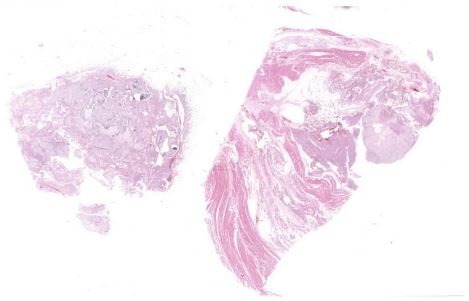

Figure 4-3: Hindlimb, African green monkey: Two sections of a multifocally mineralized bony mass within the subcutaneous fat (left) and skeletal muscle (right) are submitted for examination. (HE, 10X)

ing remodeling. Multifocally within the mineralized soft tissue lesions, multiple tortuous blood vessels with thickened tunica media were observed. Additionally, there were areas of extensive hemorrhage, neovascularization, and granulation tissue formation infiltrating and replacing the surrounding adipose tissue.

Contributing Institution:

Pathology Department, Ross University School Of Veterinary Medicine
https://veterinary.rossu.edu/research/pathology-training-program

Contributor's Morphologic Diagnosis:

Skeletal muscle: Granulomatous myositis and steatitis with soft tissue mineralization, chronic, focally extensive, severe, with fibrosis and rare osseous metaplasia.

Contributor's Comment:

Soft tissue mineralization is broadly categorized into three types based on underlying pathophysiologic mechanisms: dystrophic, metastatic, and idiopathic calcification.[5,7]

Dystrophic calcification is characterized by the deposition of mineral in areas of tissue injury, occurring despite normal serum levels of calcium and phosphate. It is often associated with prior injury, necrosis, inflammation, or neoplasia, and has been reported following chronic inflammatory conditions. Metastatic calcification occurs primarily in humans and is associated with disturbances in calcium or phosphate metabolism, most commonly hypercalcemia, hyperphosphatemia or a combination of both. It is typically observed in conditions such as chronic renal failure, end-stage kidney disease, or vitamin D toxicosis. Idiopathic calcification occurs without identifiable tissue injury or underlying metabolic abnormality. No specific cause is evident, although breed or familial predisposition may be present.[5,7]

In humans, Hyperphosphatemic Familial Tumoral Calcinosis (HFTC) results from either a deficiency of intact FGF23 or impaired FGF23 signaling, most oftenin-herited in an autosomal recessive pattern. Mutations in GALNT3, FGF23, KL (encoding KLOTHO), as well as the presence of autoantibodies targeting FGF23, disrupt FGF23 production or activity. This disruption results in hyperphosphatemia with high-normal calcium levels, leading to an

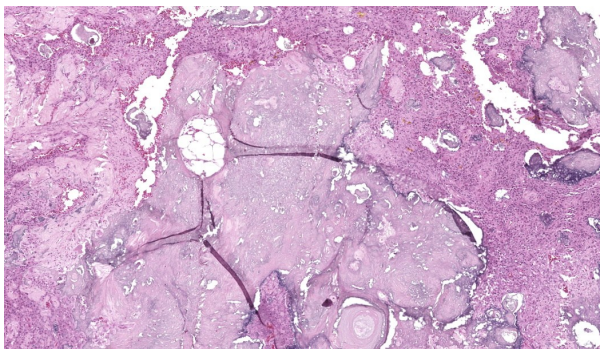

Figure 4-4: Hindlimb, African green monkey: The mass is composed of disorganized foci of mineral, fibrous connective tissue, osteoid matrix, and woven bone. (HE 176X)

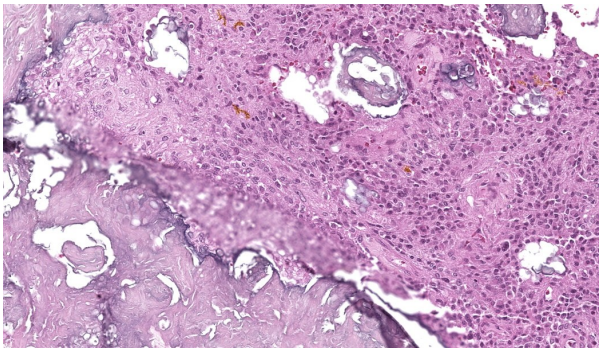

Figure 4-5: Hindlimb, African green monkey: The mass is surrounded by loosely arranged fibrous connective tissue containing numerous epithelioid macrophages. (HE, 378X)

elevated calcium-phosphate product, which is believed to play a key role in the development of ectopic calcification.[1]

In animals, gross lesions associated with calcinosis circumscripta have been documented in a variety of anatomical locations, including the tongue, margins of the pinnae, spine, salivary glands, aorta, mammary glands, small intestine, footpads, paravertebral soft tissues, cheeks, and both right and left hind limbs.[4,5,7]

In dogs, cats, and horses, the lesions typically present as bulging, fluctuant, or cystic masses that may be variably ulcerated and contain chalky white mineralized material.[4] In a study comprising 77 canine cases, lesion diameters ranged from 2 to 13 cm, with the majority measuring between 0.5 and 3 cm. Lesions were solitary in 82% of cases and multiple in 18%, with no apparent symmetry in the latter. Grossly, lesions varied from small, firm, white nodules to large cystic masses filled with abundant chalky white material. Some lesions were freely movable, whereas others were firmly adherent to the surrounding tissues. On cut surface, most lesions exhibited multifocal nodules containing gritty, chalky white material.[7]

In a documented case involving a cynomolgus macaque (*Macaca fascicularis*), multiple raised, nodular masses of variable size were observed on both, the left and right feet. On cross-section the lesions consisted of firm subcutaneous nodules containing white, chalk-like material, and no gross pathological abnormalities were identified in the internal organs.[5]

Histologically, calcinosis circumscripta is characterized by aggregates of amorphous to granular, lightly to deeply basophilic mineralized material. These deposits are typically surrounded by macrophages, multinucleated giant cells, and occasional lymphocytes, and are delineated by fibrous connective tissue bands. As the lesion progresses, mineralization becomes more extensive and is accompanied by pronounced fibrosis. The associated inflammatory response may diminish over time, and areas of osseous or cartilaginous metaplasia may develop. In certain cases, epidermal sequestration or transepidermal elimination of mineralized material may lead to ulceration.[2,3,4]

In this case, the lesions were confined to the right pelvic limb, with no evidence of involvement of other organ systems. A diagnosis of *calcinosis circumscripta* (tumoral calcinosis) was established based on the morphological, histopathological and immuno-

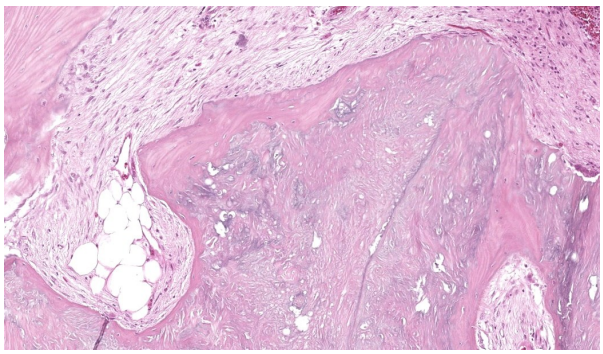

Figure 4-6: Hindlimb, African green monkey: In some areas, the mass contains woven bone. (HE, 233X)

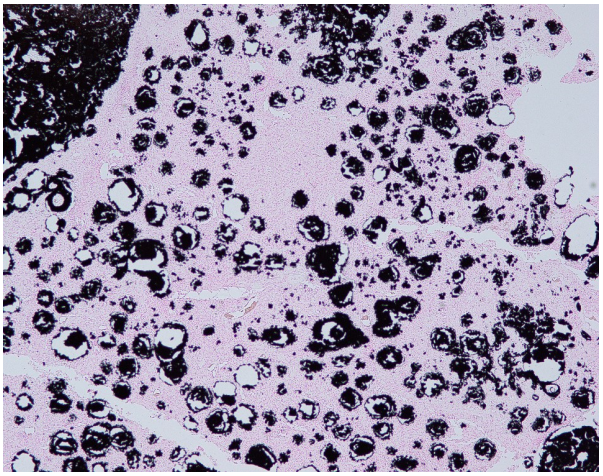

Figure 4-7: Hindlimb, African green monkey: A Von Kossa stain highlights mineral within the mass. (*Photo courtesy of*: Ross University School Of Veterinary Medicine, https://veterinary.rossu.edu/research/pathology-training-program) (Von Kossa, 100X)

histochemical characteristics of the lesion. Mason trichrome, Von Kossa and Perl's Prussian blue stains were performed and were positive for the fibrous connective tissue (the first one) and the globular amorphous mineral (the last two). The presence of iron within the mineralized material is intriguing. Anecdotally, the African Green Monkeys on this facility tend to present hepatic iron overload and multifocal organ hemosiderosis. Extraskeletal osteosarcoma was considered as a potential differential. However, the cellular infiltrate was immunopositive for IBA-1 (histiocytes/macrophages) and immunonegative for SATB2 (osteoblastic origin, osteosarcoma), α-SMA38 (mature myofibroblast, smooth muscle tumor), SOX10 (neural crest origin, melanoma and certain soft tissue neoplasms), and S100 (amelanotic melanoma and certain soft tissue neoplasms). Based on clinical history of this animal, the lesion in this case most likely represents dystrophic calcification secondary to prior traumatic injury, as has been described in other nonhuman primates. To date, neither metastatic nor idiopathic calcification has been reported in this species.

JPC Morphologic Diagnosis:

Subcutaneous fat and skeletal muscle: Mineralization, chronic, focally extensive, severe, with granulomatous inflammation and osseous metaplasia.

JPC Comment:

The lesions in this fascinating case, while most consistent with calcinosis circumscripta, also shared histologic overlap with a condition known as myositis ossificans (also known as myositis ossificans traumatica). Myositis ossificans (MO) presents as a focal mass in the skeletal muscle, most commonly associated with the limbs, such as the biceps or thigh muscles.[8] The pathogenesis of MO is speculative, but is believed to occur due to trauma and the resulting granulomatous inflammation, fibrosis, mineralization, and ossification that occur over months. Myositis ossificans is rarely reported in veterinary species, with several case reports in dogs, horses, cats, and a vampire bat.[3]

There is substantial histologic overlap between MO and calcinosis circumscripta; both lesions can have a mass effect due to mineral, fibrosis, granulomatous inflammation, and, occasionally, bone. Calcinosis circumscripta typically has a larger proportion of mineral and tends to occur in the skin and subcutis, often over pressure points. In contrast, MO has a variable amount of mineral versus bone depending on the stage of the lesion and occurs primarily within the skeletal muscle.[2] In this case, participants agreed that there were features of both present, but could not land squarely on one or the other. It is possible that the chronicity of this lesion represents a continuum between these two in

this particular case.

Participants reviewed the three main types of pathologic calcification (dystrophic, metastatic, and idiopathic) and how each relates to systemic calcium status. Dystrophic calcification occurs in necrotic or damaged tissues and is typically associated with normal serum calcium.[6] Metastatic calcification, by contrast, reflects hypercalcemia, and preferentially affects tissues involved in acid-base exchange, including the gastric lamina propria, kidneys, lungs, and blood vessels.[6] Finally, idiopathic calcification is caused by unknown metabolic triggers, but is associated with excess endogenous or exogenous corticosteroids in both veterinary and human medicine.[6]

A valuable discussion was held on the functional differences between M1 and M2 macrophages and the role of CD4+ T-helper cells in driving this differentiation. M1 macrophages, associated with pro-inflammatory responses, express CD68 and CD80, whereas M2 macrophages, associated with tissue repair and remodeling, express CD163 and CD206. Dr. Alves' lab ran these markers for this case, and the immunophenotype confirmed a predominance of M2 macrophages within the lesion. This finding aligned well with the chronicity of the process and the extensive remodeling present.
Overall, this case served as an excellent review of the mechanisms and morphologic patterns of tissue mineralization, the role of macrophage differentiation in chronic lesions, and the importance of integrating lesion distribution, chronicity, and tissue context in cases of mineralization.

References:

1. Boyce AM, Lee AE, Roszko KL, Gafni RI. Hyperphosphatemic Tumoral Calcinosis: Pathogenesis, Clinical Presentation, and Challenges in Management. *Front Endocrinol (Lausanne)*. 2020;11:293.
2. De Paolo M, Gracis M, Lacava G, Vapniarsky N, Arzi B. Management of bilateral pterygoid myositis ossificans-like lesion in dogs. Front Vet Sci. 2022 Oct 10;9:992728.
3. Hausmann JC, Manasse J, Churgin S, Steinberg H, Clyde VL, Wallace R. Myositis ossificans traumatica in a vampire bat (*Desmodus rotundus*). J Zoo Wildl Med. 2016 Sep;47(3):895-899.
4. Mauldin EA, Peters-Kennedy J. Integumentary system. In: Maxie MG, ed. *Jubb, Kennedy & Palmer's Pathology of Domestic Animals*. Vol 1. 6th ed. St. Louis: Elsevier. 2016: 509–736.
5. Radi ZA, Sato K. Bilateral dystrophic calcinosis circumscripta in a cynomolgus macaque (*Macaca fascicularis*). *Toxicol Pathol*. 2010;38(4):637-641.
6. Sakals S, Peta HG, Fernandez NJ, Allen AL. Determining the cause of hypercalcemia in a dog. *Can Vet J*. 2006;47(8):819-821.
7. Tafti AK, Hanna P, Bourque AC. Calcinosis circumscripta in the dog: a retrospective pathological study. J Vet Med A Physiol Pathol Clin Med. 2005;52(1):13-7.
8. Vilar JM, Ramirez G, Spinella G, Martinez A. Kinematic characteristics of myositis ossificans of the semimembranosus muscle in a dog. Can Vet J. 2010 Mar;51 (3):289-92.